ELSEVIER

International Journal of Heat and Fluid Flow 21 (2000) 735–739

International Journal of HEAT AND FLUID FLOW

www.elsevier.com/locate/ijhff

Effect of viscous plane stagnation flow on the freezing of fluid

Joo-Sik Yoo *

Department of Mechanical Engineering Education, Andong National University, 388 Songchun-dong, Andong, Kyungpuk 760-749, South Korea

Received 30 April 1999; accepted 29 April 2000

Abstract

This article investigates the phase-change problem from liquid to solid in the viscous plane stagnation flow. The solution at the initial stage of freezing is obtained by expanding it in powers of time, and the final equilibrium state is determined from the steady-state governing equations. The effect of the stagnation flow on the pure conduction problem can be clearly seen from the explicit analytic solutions, and the characteristics of the growth of solid and the transient heat transfer for all the dimensionless parameters are elucidated. © 2000 Elsevier Science Inc. All rights reserved.

Keywords: Viscous stagnation flow; Phase change; Freezing rate; Heat transfer

1. Introduction

Well-known forced flows which have exact solutions include the von Kármán swirling flow induced by an infinite rotating disk and the stagnation flow on an infinite plane (Schlichting, 1979). Yoo (1991, 1997) first considered the phase-change problem for the von- Kármán swirling flow, and investigated the transient heat transfer in both solid and liquid phases and the freezing rate. Subsequently, Rangel and Bian (1996) and Yoo (1999) investigated an inviscid stagnation-flow solidification problem, while Bian and Rangel (1996) also studied a viscous stagnation-flow solidification problem.

In the present study, we consider the viscous plane stagnation-flow solidification problem (Fig. 1). Initially, the fluid is kept at a uniform temperature (T_H). The temperature of the substrate is suddenly lowered below the freezing temperature and maintained constant (T_C). As a result, solidification occurs at the surface of the substrate and the solid grows with time. We obtain dimensionless governing equations which are expressed with four dimensionless parameters of Pr, θ_R/K_R, Ste, and α_R, and the characteristics of the growth of solid and the heat transfer for all the variables are elucidated from the explicit analytic solutions at the initial stage of freezing and the final equilibrium state.

2. Analysis

2.1. Governing equations

We assume that the thermophysical properties of solid and liquid phases are constant. The governing equations are described as follows (Yoo, 1991) :

$$\frac{\partial T_S}{\partial t} = \alpha_S \frac{\partial^2 T_S}{\partial y^2} \quad \text{at } 0 < y < X(t), \tag{1}$$

$$\frac{\partial T_L}{\partial t} + v[y - X(t)] \frac{\partial T_L}{\partial y} = \alpha_L \frac{\partial^2 T_L}{\partial y^2} \quad \text{at } y > X(t) \tag{2}$$

with the boundary conditions

$$K_S \frac{\partial T_S}{\partial y} - K_L \frac{\partial T_L}{\partial y} = \rho L \frac{dX}{dt} \qquad \text{at } y = X(t) \tag{3}$$

and

$$T_S = T_C \quad \text{at } y = 0, \quad T_S = T_L = T_F \quad \text{at } y = X(t),$$
$$T_L = T_H \quad \text{at } y \to \infty. \tag{4}$$

In Eq. (2), $v(y;t)$ is the velocity component in the direction normal to the solid. In the viscous plane stagnation flow (Hiemenz flow: Schlichting, 1979), the velocity is expressed as

$$v(y;t) = -\sqrt{A\nu}\,\phi(\xi,\tau), \quad \xi = \sqrt{\frac{A}{\nu}}\,y, \qquad \tau = At. \tag{5}$$

The heat fluxes at the surface of solid (Q_S) and the liquid side of solid–liquid interface (Q_L) are defined as

$$Q_S(t) = -K_S \left[\frac{\partial T_S(y,t)}{\partial y}\right] \quad \text{at } y = 0, \tag{6}$$

$$Q_L(t) = -K_L \left[\frac{\partial T_L(y,t)}{\partial y}\right] \quad \text{at } y = X(t). \tag{7}$$

Let us introduce the following dimensionless variables:

$$\zeta = \sqrt{\frac{A}{\alpha_L}}\,y, \quad \theta_S = \frac{T_S - T_C}{T_F - T_C}, \quad \theta_L = \frac{T_L - T_H}{T_F - T_H}. \tag{8}$$

---

[*] Fax: +82-571-841-1624.
E-mail address: jsyoo@andong.ac.kr (J.-S. Yoo).

PII: S0142-727X(00)00059-X

Notation

A	potential flow strain rate
b_0, b_1	constants in the expression of dimensionless solid thickness
C_S	specific heat of solid
K_S, K_L	thermal conductivity of solid and liquid, respectively
K_R	ratio of thermal conductivity, K_S/K_L
L	latent heat
Pr	Prandtl number, ν/α_L
$Q_S(t)$	heat flux at the surface of solid
$Q_L(t)$	heat flux at the liquid side of solid–liquid interface
Q_{steady}	steady-state heat flux, $Q_S(t) = Q_L(t) = Q_{steady}$ at $t \to \infty$
Ste	Stefan number, $C_S(T_F - T_C)/L$
T_S, T_L	temperature distributions in solid and liquid phases, respectively
T_C	cold temperature of solid surface
T_F	freezing temperature of liquid
T_H	initial hot temperature of liquid
t	time
$v(y,t)$	axial velocity component of fluid
$X(t)$	thickness of solid layer
X_{eq}	solid thickness at equilibrium state
y	axial coordinate
Greeks	
α_S, α_L	thermal diffusivity of solid and liquid, respectively
α_R	ratio of thermal diffusivity, α_S/α_L
$\delta(\tau)$	dimensionless solid thickness, $\delta(\tau) = \sqrt{A/\alpha_L}X(t)$
δ_{eq}	dimensionless solid thickness at equilibrium state
$\delta_\xi(\tau)$	dimensionless solid thickness, $\sqrt{A/\nu}X(t)$
ζ	dimensionless axial coordinate, $\sqrt{A/\alpha_L}y$
η	transformed coordinate, $\zeta/\delta(\tau)$
θ_L	dimensionless temperature in liquid region, $(T_L - T_H)/(T_F - T_H)$
θ_S	dimensionless temperature in solid region, $(T_S - T_C)/T_F - T_C)$
θ_R	ratio of temperature, $(T_H - T_F)/(T_F - T_C)$
$\mathrm{d}\theta_L(\delta_\xi)/\mathrm{d}\xi$	steady-state temperature gradient at the liquid side of interface
ν	kinematic viscosity
ξ	dimensionless axial coordinate, $\sqrt{A/\nu}y$
ρ	density
σ	growth parameter in Neumann problem
τ	dimensionless time, At

Eqs. (1)–(4) are written as

$$\frac{\partial\theta_S}{\partial\tau} = \alpha_R\frac{\partial^2\theta_S}{\partial\zeta^2} \quad \text{at } 0 < \zeta < \delta, \tag{9}$$

$$\frac{\partial\theta_L}{\partial\tau} - Pr^{1/2}\,\phi\left[Pr^{-1/2}(\zeta - \delta)\right]\frac{\partial\theta_L}{\partial\zeta} = \frac{\partial^2\theta_L}{\partial\zeta^2} \quad \text{at } \zeta > \delta, \tag{10}$$

$$\frac{\partial\theta_S}{\partial\zeta} + \frac{\theta_R}{K_R}\frac{\partial\theta_L}{\partial\zeta} = \frac{1}{\alpha_R\,Ste}\frac{\mathrm{d}\delta}{\mathrm{d}\tau} \quad \text{at } \zeta = \delta, \tag{11}$$

$$\begin{gathered}\theta_S = 0 \quad \text{at } \zeta = 0, \quad \theta_S = \theta_L = 1 \quad \text{at } \zeta = \delta(\tau),\\ \theta_L = 0 \text{ at } \zeta \to \infty,\end{gathered} \tag{12}$$

where

$$\delta(\tau) = \sqrt{\frac{A}{\alpha_L}}X(t) \tag{13}$$

denotes the dimensionless solid thickness. It is assumed that $\delta(0) = 0$.

Let us introduce the following coordinate transformation to fix the moving boundary of the position of solid–liquid interface $\zeta = \delta(\tau)$ at $\eta = 1$:

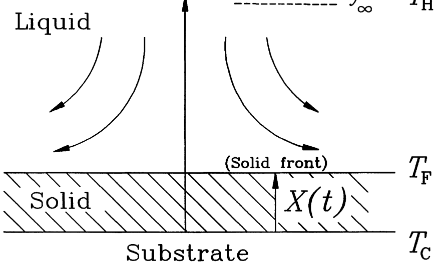

Fig. 1. Plane stagnation flow ahead of a solidifying interface.

$$\eta = \frac{\zeta}{\delta(\tau)} \tag{14}$$

Eqs. (9)–(12) are transformed as

$$\delta^2\frac{\partial\theta_S}{\partial\tau} - \frac{\eta}{2}\frac{\mathrm{d}\delta^2}{\mathrm{d}\tau}\frac{\partial\theta_S}{\partial\eta} = \alpha_R\frac{\partial^2\theta_S}{\partial\eta^2} \quad \text{at } 0 < \eta < 1, \tag{15}$$

$$\begin{aligned}&\delta^2\frac{\partial\theta_L}{\partial\tau} - \frac{\eta}{2}\frac{\mathrm{d}\delta^2}{\mathrm{d}\tau}\frac{\partial\theta_L}{\partial\eta} - Pr^{(1/2)}\delta\phi\left[Pr^{(-1/2)}(\eta - 1)\delta\right]\frac{\partial\theta_L}{\partial\eta}\\ &= \frac{\partial^2\theta_L}{\partial\eta^2} \quad \text{at } \eta > 1,\end{aligned} \tag{16}$$

$$\frac{\partial\theta_S}{\partial\eta} + \frac{\theta_R}{K_R}\frac{\partial\theta_L}{\partial\eta} = \frac{1}{2\alpha_R\,Ste}\frac{\mathrm{d}\delta^2}{\mathrm{d}\tau} \quad \text{at } \eta = 1, \tag{17}$$

$$\begin{gathered}\theta_S = 0 \quad \text{at } \eta = 0, \quad \theta_S = \theta_L = 1 \quad \text{at } \eta = 1,\\ \theta_L \to 0 \quad \text{at } \eta \to \infty.\end{gathered} \tag{18}$$

2.2. Initial stage of freezing and final equilibrium state

The initial temperature of the liquid region is uniform and is equal to T_H. Once the temperature of the substrate has been lowered to $T_C(< T_F)$, phase change from liquid to solid occurs at the surface of the solid, and the temperature front (at which $T = T_H$) moves into the liquid region as time proceeds. For the initial stage of freezing ($\tau \ll 1$), the temperature front is close to the solid–liquid interface, and the dimensionless velocity field near the wall ($\xi = \delta_\xi$) is approximated as

$$\phi(\xi,\tau) = \frac{\phi''(0)}{2}(\xi - \delta_\xi)^2 \quad \text{at } \xi > \delta_\xi, \tag{19}$$

where $\phi''(0) = 1.232588$ (Dorrepaal, 1986).

We assume that the fluid flow is quasi-steady for small time of the initial-stage freezing. This assumption is similar to that of quasi-stationarity used in the numerical computation, which assumes that the convection is in a steady state at every time step (Benard et al., 1986). Under these assumptions, the initial stage solutions, $\theta_{\mathrm{S,L}}(\tau,\eta)$ and $\delta(\tau)$, can be expanded in powers of time (Yoo, 1991, 1999):

$$\theta_{\mathrm{S,L}}(\tau,\eta) = \theta^0_{\mathrm{S,L}}(\eta) + \theta^1_{\mathrm{S,L}}(\eta)\tau^{3/2} + \cdots, \qquad (20)$$

$$\delta^2(\tau) = b_0\tau + b_1\tau^{5/2} + \cdots. \qquad (21)$$

Substitution of Eqs. (19)–(21) into Eqs. (15)–(18) yields equations for $\mathrm{O}(\tau^0)$ and $\mathrm{O}(\tau^{3/2})$, and the solutions are determined explicitly as shown in Appendix A.

The equilibrium state is determined from Eqs. (1)–(4) with $\partial/\partial t = 0$. The equilibrium solid thickness (X_{eq}) is found from the energy balance at the interface (Eq. (3) with $\mathrm{d}X/\mathrm{d}t = 0$). It gives

$$X_{\mathrm{eq}} = -\frac{K_{\mathrm{R}}}{\theta_{\mathrm{R}}}\sqrt{\frac{\nu}{A}}\left(\frac{\mathrm{d}\theta_{\mathrm{L}}(\delta_\xi)}{\mathrm{d}\xi}\right)^{-1}, \qquad (22)$$

where the temperature gradient at the liquid side of the interface, $\mathrm{d}\theta_{\mathrm{L}}(\delta_\xi)/\mathrm{d}\xi$, is a function of Pr obtained from the following equation:

$$\frac{\mathrm{d}^2\theta_{\mathrm{L}}}{\mathrm{d}\xi^2} - Pr\,\phi(\xi-\delta_\xi)\frac{\mathrm{d}\theta_{\mathrm{L}}}{\mathrm{d}\xi} = 0 \qquad (23)$$

with the boundary conditions

$$\theta_{\mathrm{L}} = 1 \quad \text{at } \xi = \delta_\xi, \qquad \theta_{\mathrm{L}} = 0 \quad \text{at } \xi \to \infty. \qquad (24)$$

3. Results and discussion

In the initial stage of solidification, the thickness of the solidified layer $\delta(\tau)$ is approximated as Eq. (21), where the first term ($b_0\tau$) represents the pure conduction solution of Neumann and the second ($b_1\tau^{5/2}$) is created by the fluid flow. Calculation shows that b_1 has negative values in all cases, which reveals that the fluid flow toward the substrate inhibits the solidification process. The effect of the fluid flow on the growth rate of the solid can be seen from the expression

$$X^2(t) = 4\sigma^2\alpha_{\mathrm{S}}t\left[1 - |b_1/b_0|\,(At)^{3/2}\right], \qquad (25)$$

in which the term $-|b_1/b_0|(At)^{3/2}$ represents the magnitude of the effect of the fluid flow on the pure conduction problem. The values of b_0, $-b_1$ and $-(b_1/b_0)$ as functions of Pr, $\theta_{\mathrm{R}}/K_{\mathrm{R}}$, Ste, and α_{R} are presented in Fig. 2.

At first, the effect of Prandtl number on the growth rate of solid is investigated (Fig. 2(a)). From the solution of $\mathrm{O}(\tau^{3/2})$, we can see that the magnitude of b_1 is inversely proportional to $\sqrt{Pr}$, which shows that the solidification rate is more strongly affected by the fluid flow in the case of a fluid with smaller Prandtl number. This is because the thickness of velocity boundary layer is proportional to $\sqrt{\nu}$.

Second, Fig. 2(b)–(d) represent the effect of temperature ratio and conductivity ratio, Stefan number, and diffusivity ratio on the growth rate of solid. The magnitude of $-(b_1/b_0)$ is increased, as $\theta_{\mathrm{R}}/K_{\mathrm{R}}$, Ste or α_{R} increases. This reveals that as the initial liquid temperature, conductivity of liquid, Stefan number, or diffusivity ratio becomes larger, the solidification rate is more strongly affected by the fluid flow.

Eq. (22) shows that the upper limit X_{eq} is independent of Ste and α_{R}. The steady-state temperature gradient $[-\mathrm{d}\theta_{\mathrm{L}}(\delta_\xi)/\mathrm{d}\xi]$ as a function of the Prandtl number is plotted in Fig. 3, which shows that $[-\mathrm{d}\theta_{\mathrm{L}}(\delta_\xi)/\mathrm{d}\xi]$ is an increasing function with respect to Pr. It was observed that the temperature gradient of $F = -\mathrm{d}\theta_{\mathrm{L}}(\delta_\xi)/\mathrm{d}\xi$ could be closely approximated as $F = 0.57\,Pr^{0.438}$ for $Pr < 1$, and $F = 0.57\,Pr^{0.359}$ for $Pr > 1$, within 5% error. And from Eq. (22), we can see that X_{eq} is a decreasing function of Pr.

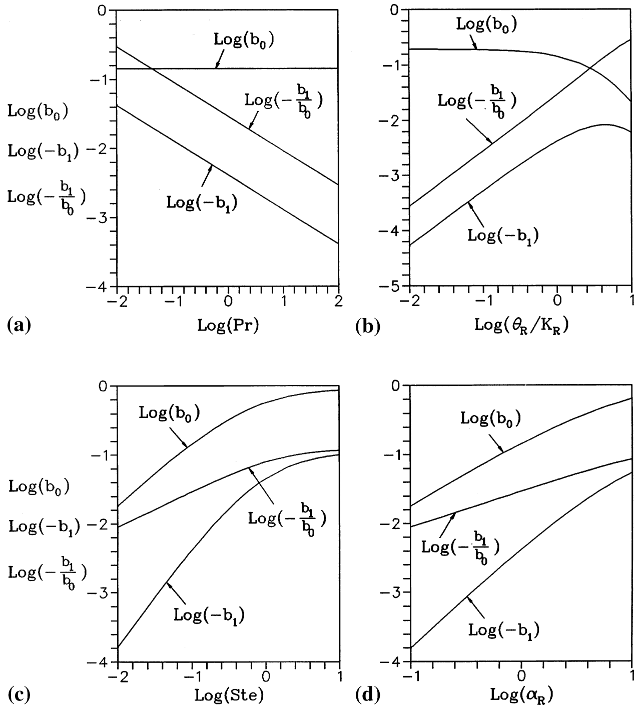

Fig. 2. Effect of several parameters on the growth rate of solid: (a) effect of Prandtl number (Pr) with $\alpha_{\mathrm{R}} = \theta_{\mathrm{R}}/K_{\mathrm{R}} = 1$ and $Ste = 0.1$; (b) effect of temperature ratio (θ_{R}) and conductivity ratio (K_{R}) with $\alpha_{\mathrm{R}} = Pr = 1$ and $Ste = 0.1$; (c) effect of Stefan number (Ste) with $\alpha_{\mathrm{R}} = Pr = \theta_{\mathrm{R}}/K_{\mathrm{R}} = 1$; (d) effect of diffusivity ratio (α_{R}) with $Pr = \theta_{\mathrm{R}}/K_{\mathrm{R}} = 1$ and $Ste = 0.1$.

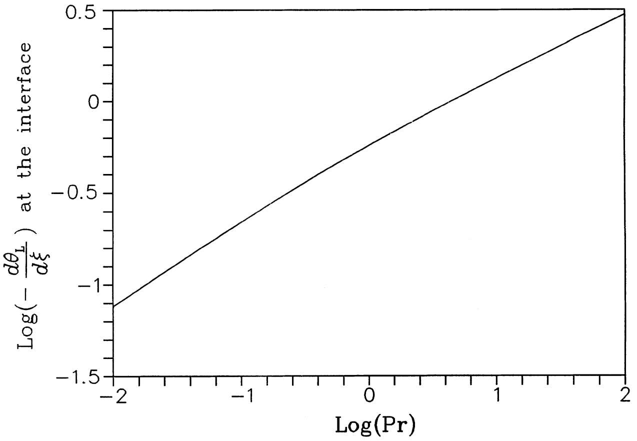

Fig. 3. Steady-state temperature gradient at the liquid side of solid–liquid interface, $-\mathrm{d}\theta_{\mathrm{L}}(\delta_\xi)/\mathrm{d}\xi$, as a function of the Prandtl number (Pr).

The transient behavior of the heat fluxes, $Q_{\mathrm{S}}(\tau)/Q_{\mathrm{steady}}$ and $Q_{\mathrm{L}}(\tau)/Q_{\mathrm{steady}}$, for several parameters is shown in Figs. 4–6. At first, Fig. 4 shows that as Pr increases, both $Q_{\mathrm{S}}(\tau)/Q_{\mathrm{steady}}$ and $Q_{\mathrm{L}}(\tau)/Q_{\mathrm{steady}}$ are increased, that is, the response time of heat transfer in both solid and liquid phases is increased. The general trend of $Q_{\mathrm{L}}(\tau)/Q_{\mathrm{steady}}$ for Prandtl numbers shown in Fig. 4(a) is similar to that of the case when there is no phase change (Chao and Jeng, 1965; Sano, 1981). However, the characteristics for the heat fluxes are different from those

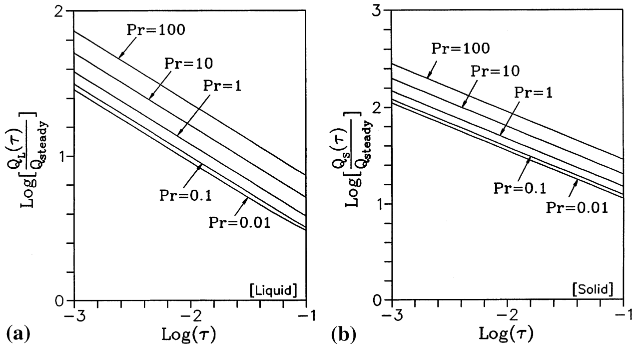

Fig. 4. Transient heat fluxes at the surface of solid (Q_S) and the liquid side of solid–liquid interface (Q_L) for several values of *Pr* with $\alpha_R = \theta_R/K_R = 1$ and $Ste = 0.1$: (a) $Q_L(\tau)/Q_{steady}$; (b) $Q_S(\tau)/Q_{steady}$.

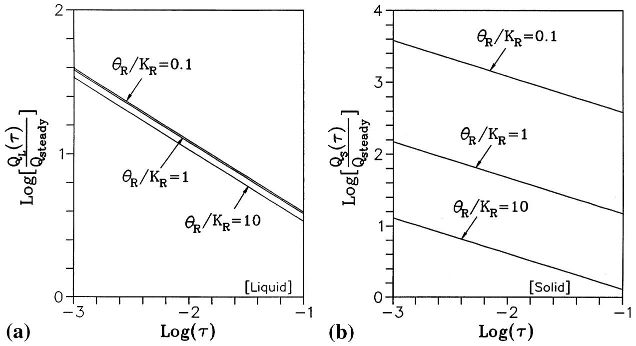

Fig. 5. Transient heat fluxes at the surface of solid (Q_S) and the liquid side of solid–liquid interface (Q_L) for several values of θ_R/K_R with $\alpha_R = Pr = 1$ and $Ste = 0.1$: (a) $Q_L(\tau)/Q_{steady}$; (b) $Q_S(\tau)/Q_{steady}$.

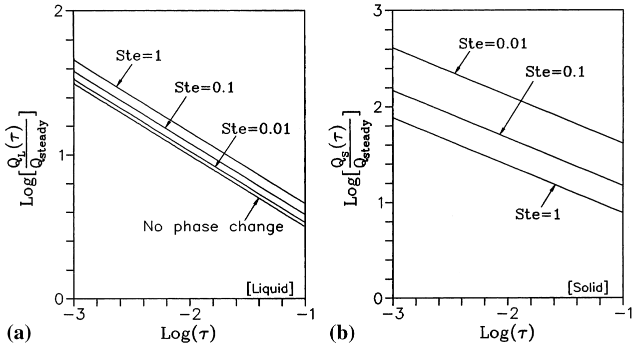

Fig. 6. Transient heat fluxes at the surface of solid (Q_S) and the liquid side of solid–liquid interface (Q_L) for several Stefan numbers (*Ste*) with $\alpha_R = Pr = \theta_R/K_R = 1$, and Q_L for the case with no phase change: (a) $Q_L(\tau)/Q_{steady}$; (b) $Q_S(\tau)/Q_{steady}$.

observed in the rotating-disk-revolving system, in which the minimum in response time occurs around $Pr = 1$ (Yoo, 1997).

For θ_R/K_R (Fig. 5), both $Q_S(\tau)/Q_{steady}$ and $Q_L(\tau)/Q_{steady}$ are decreased with increased value of θ_R/K_R, since the maximum solid thickness (δ_{eq}) that can be grown is inversely proportional to θ_R/K_R.

Finally, Fig. 6 shows the dependency of the heat fluxes on *Ste*. When phase change is present, $Q_L(\tau)/Q_{steady}$ is larger than that for the case with no phase change and the difference increases with increase of *Ste*. The dependency of the heat fluxes on the variable α_R showed the same characteristics as that for *Ste*.

In summary, the transient solution of the dimensionless governing equations is dependent on the four dimensionless parameters of *Pr*, θ_R/K_R, *Ste*, and α_R, but the equilibrium state is dependent on only the two parameters of *Pr* and θ_R/K_R.

Appendix A

Equations for $O(\tau^0)$:

$$\frac{d^2\theta_S^0}{d\eta^2} + \frac{b_0}{2\alpha_R}\eta\frac{d\theta_S^0}{d\eta} = 0 \quad \text{at } 0 < \eta < 1, \tag{A.1}$$

$$\frac{d^2\theta_L^0}{d\eta^2} + \frac{b_0}{2}\eta\frac{d\theta_L^0}{d\eta} = 0 \quad \text{at } \eta > 1, \tag{A.2}$$

$$\frac{d\theta_S^0}{d\eta} + \frac{\theta_R}{K_R}\frac{d\theta_L^0}{d\eta} = \frac{b_0}{2\alpha_R\, Ste} \quad \text{at } \eta = 1, \tag{A.3}$$

$$\theta_S^0(0) = 0, \quad \theta_S^0(1) = \theta_L^0(1) = 1, \quad \theta_L^0(\infty) = 0. \tag{A.4}$$

Equations for $O(\tau^{3/2})$:

$$\frac{d^2\theta_S^1}{d\eta^2} + \frac{b_0}{2\alpha_R}\eta\frac{d\theta_S^1}{d\eta} - \frac{3b_0}{2\alpha_R}\theta_S^1 = -\frac{5b_1}{4\alpha_R}\eta\frac{d\theta_S^0}{d\eta} \quad \text{at } 0 < \eta < 1, \tag{A.5}$$

$$\frac{d^2\theta_L^1}{d\eta^2} + \frac{b_0}{2}\eta\frac{d\theta_L^1}{d\eta} - \frac{3b_0}{2}\theta_L^1 = -\left[\frac{\phi''(0)}{2}\, Pr^{-(1/2)}\, b_0^{(3/2)}(\eta - 1)^2 + \frac{5b_1}{4}\eta\right]\frac{d\theta_L^0}{d\eta} \quad \text{at } \eta > 1, \tag{A.6}$$

$$\frac{d\theta_S^1}{d\eta} + \frac{\theta_R}{K_R}\frac{d\theta_L^1}{d\eta} = \frac{5b_1}{4\alpha_R\, Ste} \quad \text{at } \eta = 1, \tag{A.7}$$

$$\theta_S^1(0) = \theta_S^1(1) = \theta_L^1(1) = \theta_L^1(\infty) = 0. \tag{A.8}$$

The solution of Eqs. (A.1)–(A.4) for $O(\tau^0)$ is the Neumann solution (Carslaw and Jaeger, 1959):

$$\theta_S^0(\eta) = \frac{\operatorname{erf}(\sigma\eta)}{\operatorname{erf}(\sigma)}, \tag{A.9}$$

$$\theta_L^0(\eta) = \frac{\operatorname{erfc}(\sigma\sqrt{\alpha_R}\eta)}{\operatorname{erfc}(\sigma\sqrt{\alpha_R})}, \tag{A.10}$$

$$\frac{\exp(-\sigma^2)}{\operatorname{erf}(\sigma)} - \frac{\theta_R\sqrt{\alpha_R}\,\exp(-\sigma^2\alpha_R)}{K_R\operatorname{erfc}(\sigma\sqrt{\alpha_R})} = \frac{\sqrt{\pi}\sigma}{Ste}, \tag{A.11}$$

$$b_0 = 4\sigma^2\alpha_R. \tag{A.12}$$

The solution of Eqs. (A.5)–(A.8) is found with a homogeneous solution of the form

$$u_S(\eta) = \eta^3 + \frac{3}{2\sigma^2}\eta, \tag{A.13}$$

$$u_L(\eta) = \eta^3 + \frac{3}{2\sigma^2\alpha_R}\eta. \tag{A.14}$$

The solution is

$$\theta_{\mathrm{S}}^{1}(\eta) = -u_{\mathrm{S}}(\eta)\int_{\eta}^{1} \frac{b_1 C_1 g(\eta)}{\exp(\sigma^2\eta^2)u_{\mathrm{S}}^2(\eta)}\,\mathrm{d}\eta, \tag{A.15}$$

$$\theta_{\mathrm{L}}^{1}(\eta) = u_{\mathrm{L}}(\eta)\int_{1}^{\eta} \frac{(C_3/\sqrt{Pr})f(\eta) + b_1 C_2 h(\eta) + C_4}{\exp(\sigma^2\alpha_{\mathrm{R}}\eta^2)u_{\mathrm{L}}^2(\eta)}\,\mathrm{d}\eta, \tag{A.16}$$

where the functions $f(\eta)$, $g(\eta)$, and $h(\eta)$ are defined as

$$f(\eta) = \frac{\eta^6}{6} - \frac{2}{5}\eta^5 + \frac{1}{4}\left(1 + \frac{3}{2\sigma^2\alpha_{\mathrm{R}}}\right)\eta^4 - \frac{1}{\sigma^2\alpha_{\mathrm{R}}}\eta^3 + \frac{3}{4\sigma^2\alpha_{\mathrm{R}}}\eta^2,$$

$$g(\eta) = \frac{\eta^5}{5} + \frac{\eta^3}{2\sigma^2}, \qquad h(\eta) = \frac{\eta^5}{5} + \frac{\eta^3}{2\sigma^2\alpha_{\mathrm{R}}}.$$

The constants b_1 and C_1–C_4 are determined explicitly by boundary conditions (A.7) and (A.8). The processes are straightforward, and the detailed equations are omitted for brevity.

References

Benard, C., Gobin, D., Zanoli, A., 1986. Moving boundary problem: heat conduction in the solid phase of a phase-change material during melting driven by natural convection in the liquid. Int. J. Heat Mass Transfer 29, 1669–1681.

Bian, X., Rangel, R.H., 1996. The viscous stagnation-flow solidification problem. Int. J. Heat Mass Transfer 39, 3581–3594.

Carslaw, H.S., Jaeger, J.C., 1959. Conduction of Heat in Solids, 2nd ed. Clarendon Press, Oxford, pp. 282–296.

Chao, B.T., Jeng, D.R., 1965. Unsteady stagnation point heat transfer. J. Heat Transfer 87, 221–230.

Dorrepaal, J.M., 1986. An exact solution of the Navier–Stokes equation which describes non-orthogonal stagnation-point flow in two-dimensions. J. Fluid Mech. 163, 141–147.

Rangel, R.H., Bian, X., 1996. The inviscid stagnation-flow solidification problem. Int. J. Heat Mass Transfer 39, 1591–1602.

Sano, T., 1981. Unsteady stagnation point heat transfer with blowing or suction. J. Heat Transfer 103, 448–452.

Schlichting, H., 1979. Boundary Layer Theory, 7th ed. McGraw-Hill, New York, 1979, pp. 95–99.

Yoo, J.-S., 1991. Effect of fluid flow induced by a rotating disk on the freezing of fluid. Int. J. Heat Fluid Flow 12, 257–262.

Yoo, J.S., 1997. Unsteady heat transfer from a rotating disk with solidification. Numer. Heat transfer, Part A 31, 765–781.

Yoo, J.-S., 1999. Effect of inviscid stagnation flow on the freezing of fluid – a theoretical analysis. Int. J. Heat Mass Transfer 42, 3707–3714.